A probabilistic study on seismic induced accumulated plastic strain

Axel Méric, Pierre Labbé, Djaffar Boussaa, Jean-François Semblat, Pierre-Alain Nazé

TINCE 2023 – Technological Innovations in Nuclear Civil Engineering

A probabilistic study on seismic induced accumulated plastic strain

Axel Méric [1*], Pierre Labbé [2], Djaffar Boussaa [3], Jean-François Semblat [4], Pierre-Alain Nazé [1]

[1]Geodynamique & Structure, Montrouge, France; [2]IRC, ESTP Paris, Cachan, France; [3]LMA AMU CNRS Centrale (UMR7031), Marseille, France; [4]IMSIA (UMR9219), CNRS, EDF, CEA, ENSTA Paris, Institut Polytechnique de Paris, France.

[*] Corresponding Author, E-mail: axel.meric@geodynamique.com

Abstract: A linearization method based on the work of Nguyen *[Analyse systématique du concept de comportement linéaire équivalent en ingénierie sismique, PhD., université Paris-Est; EDF; ESTP, Cachan (2017)]* is extended in this paper. The method is based on the fitting of the relative acceleration transfer function of a linear SDOF oscillator on non-linear relative acceleration transfer functions to obtain the equivalent dynamic parameters in terms of frequency and viscous damping ratio. This paper proposes formulas for the fitting and introduces an additional parameter in the non-linear transfer function numerical calculation. Elastic perfectly plastic, linear kinematic hardening and non-linear kinematic hardening materials behaviors are considered. The cases of wide and narrow band input motions are explored. The linearization method results are compared to formulas from the literature and evaluated according to goodness of fit criteria. The method gives good results regarding relative speed and acceleration values and less accurate results regarding the maximum displacement prediction. This method should be considered in the case of the determination of transferred motions and fatigue analysis.

KEYWORDS: Accumulated strain, Linearization, Earthquake, Random process.

Introduction

For a structure or a mechanical system, a seismic input motion can be regarded as an imposed cyclic load history. If the input is strong enough, it can induce irreversible changes because the system evolves out of its reversible domain. Moreover, as the input motion is a succession of cycles, the system accumulates irreversible changes at each cycle, this is specially the case when a permanent force (gravity, pressure) applies in addition to the seismic input motion. Here are some examples of this phenomenon that were already studied:

- Accumulation of seismically induced sliding of gravity dams, where the reservoir water pressure acts as a permanent force (Labbé, 2023);
- Accumulation of seismically induced settlements of a soil column overlying a bedrock during an earthquake, where gravity acts as a permanent force. This problem was studied by Vincens et al (2003) who proposed a settlement predictive formula;
- Accumulation of circumferential plastic strain (ratcheting) in straight pressurized pipes under seismically induced cycles of torsion, where pressure is a permanent load. This was studied by Boussaa and Labbé (1992) who proposed a formula to approximate ratcheting.

These kinds of mechanical problems can be modeled by elastic-plastic SDOF or MDOF oscillators and have been studied thoroughly in the last decades. Many linearization techniques and formulas have been proposed. The first notable study is the one by Caughey (1960) who explored the steady-state response of the hysteretic oscillator under harmonic forces. Iwan and Paparizos (1988) studied the response of strongly yielding oscillators and showed their frequency shift when they are strained out of their linear domain. They also highlighted the importance of the response content at low frequency regarding the prediction of the plastic drift. Following the idea of Karnopp and Scharton (1966), Paparizos and Iwan (1988) studied the non-linear part of the elastic-plastic oscillator response as a “plastic process” viewed as a Brownian motion. They proposed formulas for the plastic drift response statistics. From this concept, Borsoi and Labbé (1989) derived a method to determine the probability of collapse of elastic-perfectly plastic oscillators excited by white-noise type input motions. Later, from the same paradigm, Feau (2008) proposed a formula for the mean ductility demand. Formulas for frequency shift ratio and equivalent viscous damping ratio were also proposed by Jacobsen (1930), Reddy and Pratap (2000), Blandon (2005) and more recently by Liu et al. (2014 and 2015).

Other methods are also found in the literature, such as in the series of article of Bouc and Boussaa (1998, 2001, 2002). They derived formulas for the mean drift response of the elastic-perfectly plastic oscillator under zero and non-zero mean random load, through resolution of the stochastic equation of motion, where the motion is decomposed into a non-stationary drift term and a stationary oscillatory term. More recently, Boussaa and Bouc (2018) refined the method to propose satisfactory prediction of the elastic-perfectly plastic oscillator's velocity power spectral density under wide-band random excitations.

This article follows in the footsteps of papers by Nguyen (2017) and by Labbé & Nguyen (2019, 2020 and 2021) who studied the margins of non-linear oscillators under zero-mean wide band random excitation and highlighted the importance of the input motion frequency content. They also proposed a linearization method which consists in finding the equivalent dynamic parameters (equivalent resonance frequency and equivalent viscous damping ratio) by fitting the relative acceleration transfer function of the linear oscillator on the numerical transfer function of the non-linear oscillator. This work extends and improves this method by proposing an additional parameter introduced at the denominator of the non-linear transfer function calculation and by testing three fitting formulas. Moreover, the method is applied to more situations. Different plastic behaviors (from perfectly plastic to non-linear kinematic hardening), zero and non-zero imposed initial static force, and wide band and narrow band input motions are studied. The method is evaluated by goodness of fit criteria. In the literature, most of the linearization methods aim to find a good relative displacement estimate. This is not the goal of this paper. It rather aims to obtain good predictions of the relative acceleration and relative speed non-linear responses. It finds its interest in civil engineering studies to obtain transferred motions or to perform fatigue analysis.

Considered input motions

Different types of input motions are considered in this paper: wide-band signals, representing rock site ground level seismic input motions and narrow-band signals representing the seismic motion filtered by a structure. Signals are defined by their power spectral density (PSD), which consists in the filtering of a one-sided truncated white noise, denoted by S_0, defined on the [0 Hz, 50 Hz] frequency interval.

As proposed by Nguyen (2017), this white noise is filtered by a Kanai-Taijimi (1960) filter, a Clough and Penzien (1975) filter to reduce the low frequency content of the motion, and a low-pass filter to control the high frequency content. The resulting PSD is expressed below, with H_{CP} and H_{LP} being respectively the Clough and Penzien and low-pass filter transfer functions:

$$S(\omega) = \frac{1 + 4\xi_{KT}^2\Omega_{KT}^2}{(1-\Omega_{KT}^2)^2 + 4\xi_{KT}^2\Omega_{KT}^2} |H_{CP}|^2 |H_{LP}|^2 S_0 \quad (1)$$

with:

$$H_{CP}(\omega) = \frac{\Omega_{CP}^2}{(1-\Omega_{CP}^2) + 2i\xi_{CP}\Omega_{CP}} \quad (2)$$

$$H_{LP}(\omega) = \frac{1/\omega_{LP}^2}{(\Omega_{LP}^2 - 1) + 2i\xi_{LP}\Omega_{LP}} \quad (3)$$

$$\Omega_{KT} = \frac{\omega}{\omega_{KT}} ; \Omega_{CP} = \frac{\omega}{\omega_{CP}} ; \Omega_{LP} = \frac{\omega}{\omega_{LP}} ; \omega = 2\pi f$$

The signal generation procedure is described in Labbé (2021). Each sample $\gamma_i(t)$ last 20 seconds and the strong phase of each signal is controlled by a time-envelope curve $E(t)$ of α-type (Jennings, et al., 1968) whose expression is:

$$E(t) = \alpha_1 t^{(\alpha_2 - 1)} \exp(-\alpha_3 t) \quad (4)$$

The $\gamma_i(t)$ samples correspond to the wide band input motions. To obtain narrow band input motions, we considered a simple five story structure represented in figure 1 which plays the role of a filter. Each story has the same stiffness k_s. The motion $\gamma_i(t)$ is the ground motion. Then, we calculate the relative

acceleration response $\gamma_{fi}(t)$ at the fifth story, only controlled by the structure first mode of frequency f_1 and modal linear viscous damping ξ_1. This response is our considered narrow band input. The wide band and narrow band input motions characteristics are summed up in table 1.

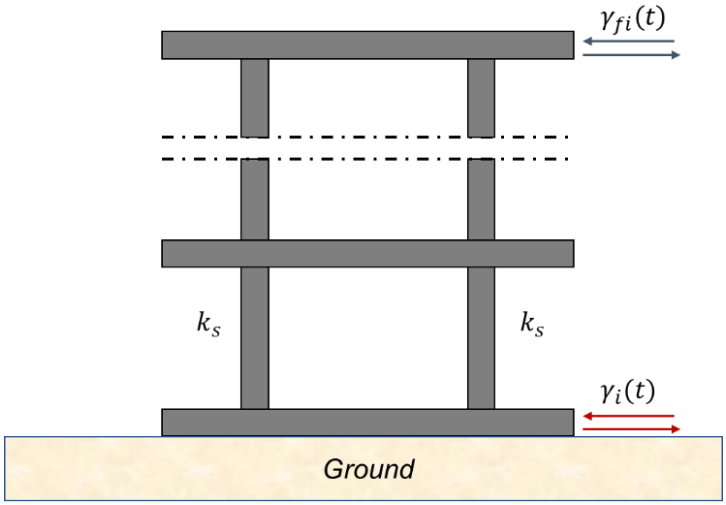

Figure 1: Five story structure filter

-	Parameter	Value	Unit
Frequency range	-	0.05 - 50	[Hz]
Kanai-Tajimi filter	f_{KT}	2.5	[Hz]
	ξ_{KT}	0.5	[-]
Clough and Penzien filter	f_{CP}	0.125	[Hz]
	ξ_{CP}	1	[-]
Low-pass filter	f_{LP}	10	[Hz]
	ξ_{LP}	1	[-]
Time envelope curve	α_1	1.33	[-]
	α_2	2.5	[-]
	α_3	0.5	[-]
Structure to obtain narrow band signals	Number of story	5	[-]
	k_s	75000000	[N/m]
	ξ_1	0.05	[-]
	f_1	3.2	[Hz]

Table 1: Input motions parameters

The statistics of the signals, more precisely, the central frequency, the peak frequency and the band-width, are studied. One thousand samples of wide and narrow band signals are respectively generated. The mean PSDs are represented in figure 2, the mean pseudo acceleration response spectra are shown in figure 3. The amplitude values are normed.

Noting m_i the spectral moment of order i of a stationary random process with zero mean, we use the Rice formula to obtain the central frequency of the PSD input motions:

$$f_c = \frac{1}{2\pi}\sqrt{\frac{m_2}{m_0}} \tag{5}$$

The proposed bandwidth measure determines the “frequency standard deviation” which corresponds to the square root of the difference between the squared PSD central frequency and the squared PSD peak frequency. The higher the standard deviation is, the wider the process bandwidth is (Preumont,

1994; Vanmarcke 1984). The measure is denoted by δ_1 :

$$\delta_1 = \sqrt{1 - \frac{m_1^2}{m_0 m_2}} \tag{6}$$

It indicates a narrow band process when the value is close to zero and a wide band process at a value close to one. The values of the central frequency, the peak frequency and the bandwidths are calculated on the mean PSDs obtained from the one thousand samples. The results are reported in table 2.

Parameter	Unit	Wide band signal	Narrow band signal
Cenral frequency	[Hz]	3.17	3.35
Peak frequency	[Hz]	2.20	3.2
Bandwidth δ_1	[-]	0.59	0.19

Table 2: Input motion statistics

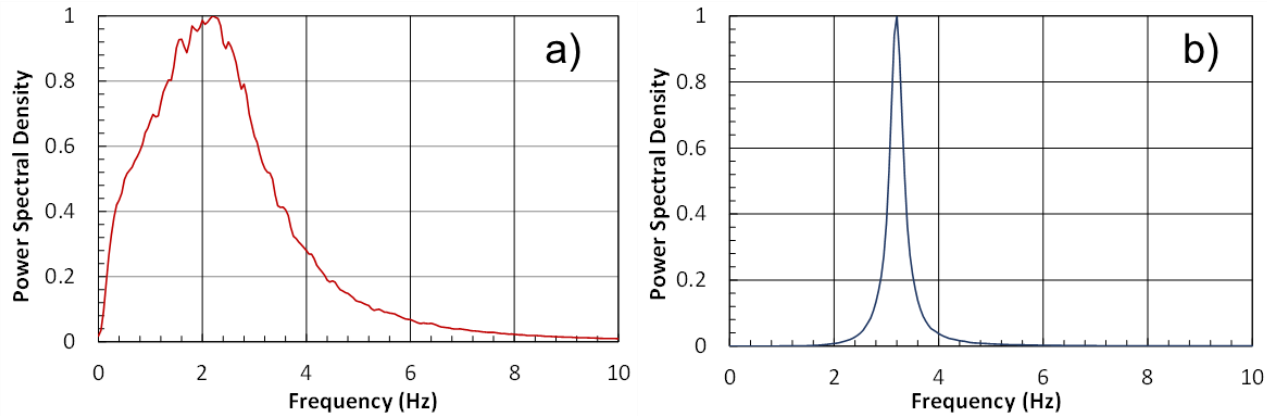

Figure 2: Mean PSD of: a) Wide band signals, b) Narrow band signals

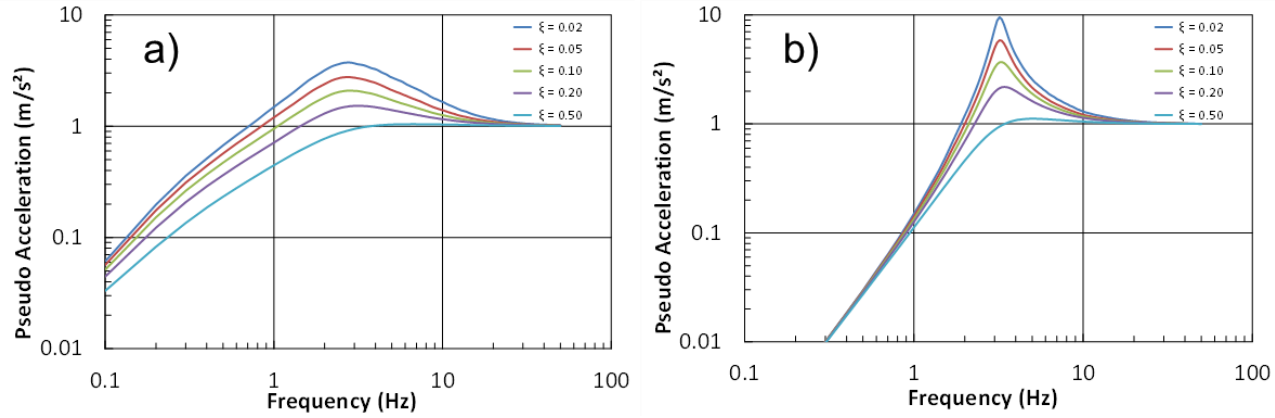

Figure 3: Mean pseudo acceleration response spectrum of: a) Wide band signals, b) Narrow band signals

The Elastic-Plastic Oscillator

Material Behavior:

As mentioned, the mechanical system that is considered here is the non-linear single degree of freedom oscillator. Its equation of motion is:

$$\ddot{X}_{tot} + 2\beta\omega_0\dot{X}_{tot} + F(X_{tot}) = -\gamma(t) \tag{7}$$

Where X_{tot} is the total displacement, β the viscous damping ratio, ω_0 the circular frequency, F the spring force and γ the input motion which can be a sample of a wide band or a narrow band signal as defined previously. By noting X_e the elastic displacement and X_p the plastic displacement, we obtain the following additive decomposition:

$$X_{TOT} = X_e + X_p \tag{8}$$

Then, the force F can be written as:

$$F(X_{tot}) = \omega_0^2\left(X_{tot} - X_p\right) \tag{9}$$

Different behaviors are considered in this paper. They are all independent of time dissipative behaviors. This choice is often made for the study of metallic materials such as steel, the studied plastic laws are listed below, with the definition of the Von-Mises yield criteria f and their flow rule $\dot{X}_P$ in the case of one-dimensional plasticity.

Perfect plasticity (EPP):

$$f = |F| - F_0 \tag{10}$$

$$\dot{X}_p = \lambda\, sign(F) \tag{11}$$

Linear Kinematic Hardening (LKH) or the so-called Prager model (1955):

$$f = |F - q| - F_0 \tag{12}$$

$$\dot{X}_p = \lambda\, sign(F - q) \tag{13}$$

$$\dot{q} = H\dot{X}_p \tag{14}$$

Non-Linear Kinematic Hardening (NLKH) or the so-called Armstrong-Frederick model (1966):

$$f = |F - q| - F_0 \tag{15}$$

$$\dot{X}_p = \lambda\, sign(F - q) \tag{16}$$

$$\dot{q} = C\dot{X}_p - \mu q\left|\dot{X}_p\right| \tag{17}$$

The complementarity conditions, $\lambda \geq 0, f \leq 0, \lambda f = 0$, apply for these three models.
In the above, F_0 is the yield force, λ the plastic multiplier, q the elasticity domain translation. H, C and μ are parameters model. These three models were chosen because they do no exhibit the same accumulation of plastic strain, or here, plastic displacement. The perfect plasticity model is known to be the least conservative one and it exhibits ratcheting at asymptotic behavior when the system is loaded by a non-zero mean cyclic force. On the contrary, the LKH model is known to only manifest elastic or plastic shakedown when the asymptotic behavior is reached, even under non-zero mean cyclic force. The NLKH model was made to propose a better representation of the stress-strain curve but also to give a more precise evaluation of the ratcheting strain, one which is overall more satisfactory than the perfect plasticity model in this regard. The literature is full of information on this subject, one could argue on the precision of the NLKH model and on its tendency to be conservative or not and that's why many models

were invented later on such as the Chaboche one (1989 and 1991). This article does not aim to critic or evaluate the precision of these models. More information can be found in the works of Lemaitre and Chaboche (1988) and of Maitournam (2019). Other model, such as models with damage, will be considered in future works.

Parameters values:

For all the calculations, the linear viscous damping ratio β is always chosen to be equal to 5%. For the EPP and LKH models, the initial oscillator stiffness k_0 varies regarding the central frequency of the input motion sample. The value H of the LKH model is chosen to be 10% of k_0. For the NLKH model, the values found in Lemaitre and Chaboche (1988) are chosen and fixed to simulate a 316 L steel, $k_0 = 210\,000$ MN, $C = 30\,000$ MN, $\mu = 60$, $F_0 = 300$ MN. In this study, for each sample, the natural frequency of the oscillator is tuned to be equal to the central frequency of the input motion γ_i or γ_{fi} such as $\frac{f_0}{f_c} = 1$.

Numerical resolution:

The chosen temporal numerical scheme is the mean acceleration implicit gamma beta Newmark scheme. The time step is 0.001s. The plasticity step is solved by a predictor-corrector algorithm. More information for the case of 1D plasticity can be found in Yaw (2017). All the calculations and algorithms were done with Python 3.

Example of results:

Equation (8) separates the elastic and the plastic part of the total displacement. It also separates the stationary oscillatory part which is the elastic displacement and the non-stationary non oscillatory part, the plastic displacement. The plastic displacement can be interpreted as a drift of the total displacement. Under a non-zero mean input motion, the system accumulates more plastic displacement at each cycle. This effect is called ratcheting, the force-displacement curve translates in the plastic flow direction after each cycle. An example is presented in the case of the NLKH oscillator. A sample of its total displacement response is obtained for a zero mean wide band input motion $\gamma_i(t)$ (see figure 4). Its response is also obtained for the same input motion, but in the case of a non-zero mean force equals to two-third of the yield strength F_0. This response is represented in figure 5, highlighting the ratcheting effect.

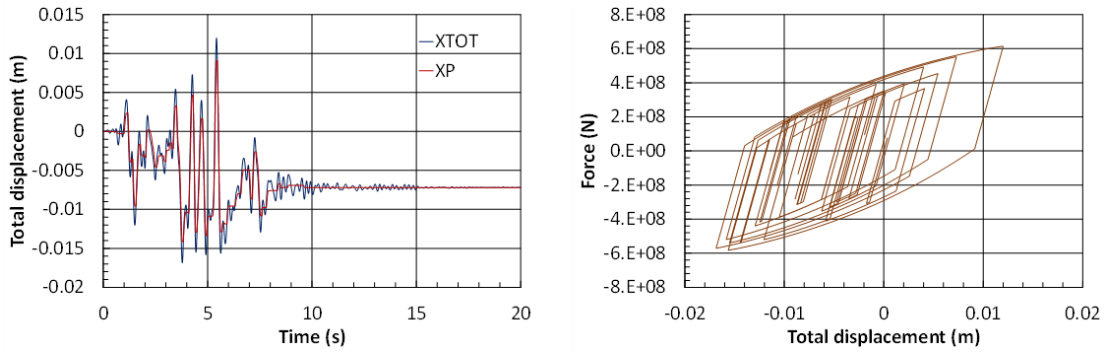

Figure 4: Sample of the NLKH oscillator response under a zero mean wide band input motion

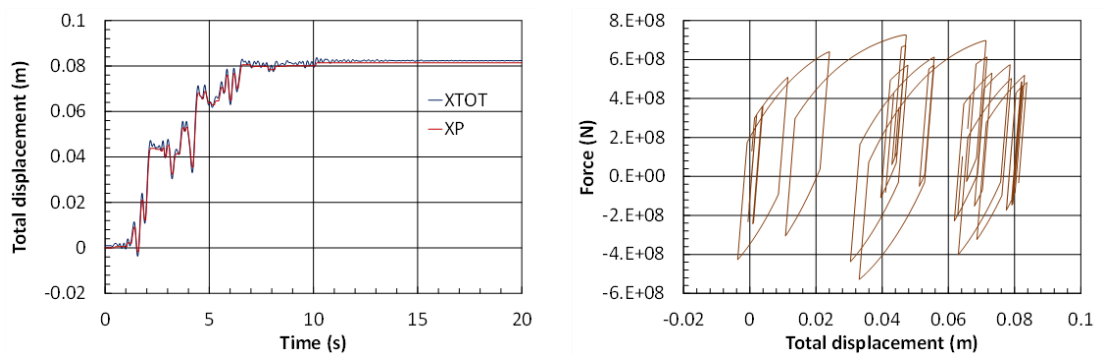

Figure 5: Sample of the NLKH oscillator response under a non-zero mean wide band input motion

Equivalent linearization by transfer function

This part focuses on the improvement of the proposed linearization method described in Nguyen (2017). This method aims to determine the equivalent dynamic parameters, the equivalent resonant frequency f_{eq} and the equivalent viscous damping ratio ξ_{eq}, by fitting the linear relative acceleration transfer function (RATF) on the numerical non-linear RATF. The choice of the RATF over the relative displacement transfer function (RDTF) has been made because of the zero-frequency content high value of the relative displacement response PSD. This specificity has already been discussed by Iwan and Paparizos (1988). It would perturb the fitting or make it impossible. The RATF formula is:

$$H_{lin}(\omega) = \frac{-\omega^2}{-\omega^2 + 2i\beta\omega_0\omega + \omega_0^2} \tag{18}$$

In the above, the parameters have the same meaning as in equation (7). The numerical RATF is noted H_{exp}. It is obtained by calculating the ratio of the relative acceleration response Fourier transform $\mathcal{F}_{exp}$ over the Fourier transform of the input motion $\mathcal{F}_{inp}$. Zero-padding is used to obtain better accuracy. In this ratio is added an "epsilon" value which is an additional parameter added at the denominator in order to reduce some non-physical peak that could appear because of the numerator that would be divided by an almost zero value. Three real epsilon values and three complex epsilon values are chosen. The case of no epsilon value is also treated. Thus, seven transfer functions are calculated per sample of response. We note H_{Cexpj}, H_{Rexpj} H_{exp0} respectively the numerical transfer functions obtained with a complex, a real and no epsilon parameter. Below are their expressions:

$$H_{Cexp\alpha}(\omega) = \frac{\mathcal{F}_{exp}(\omega)}{\alpha(1+i)\max(\mathcal{F}_{inp}) + \mathcal{F}_{inp}(\omega)} \tag{19}$$

$$H_{Rexp\alpha}(\omega) = \frac{\mathcal{F}_{exp}(\omega)}{\alpha\max(\mathcal{F}_{inp}) + \mathcal{F}_{inp}(\omega)} \tag{20}$$

$$\alpha = [0.01\,;0.02\,;0.05\,]$$

$$H_{exp0} = \frac{\mathcal{F}_{exp}(\omega)}{\mathcal{F}_{inp}(\omega)} \tag{21}$$

The fitting consists in finding the pair $(f_{eq}\,;\,\xi_{eq})$ that minimizes the difference between H_{lin} and H_{exp}. Inspired by Nugyen (2017), we propose three functions Δ_i to minimize:

$$\Delta_1 = \sum_{n=f_{min}}^{f_{max}} \left(\left(Re\left(H_{exp}(n)\right) - Re\left(H_{lin}(n)\right) \right)^2 + \left(Im\left(H_{exp}(n)\right) - Im\left(H_{lin}(n)\right) \right)^2 \right)^2 \tag{22}$$

$$\Delta_2 = \sum_{n=f_{min}}^{f_{max}} \left(\left|H_{exp}(n)\right| - \left|H_{lin}(n)\right| \right)^2 \tag{23}$$

$$\Delta_3 = \sum_{n=f_{min}}^{f_{max}} \left(Re\left(H_{exp}(n)\right) - Re\left(H_{lin}(n)\right) \right)^2 + \left(Im\left(H_{exp}(n)\right) - Im\left(H_{lin}(n)\right) \right)^2 \tag{24}$$

The Levenberg-Marquardt algorithm is applied for the mean-squares minimization problem. The lmfit python module is used, the tolerance is 1.50 10E-08, the default value.

There are three functions tested, we call M_i the method of fitting that minimizes the function Δ_i. For each method, there are seven numerical transfer function to fit. It raises to 21 the number of fit per sample of response to an input mention. To determine which method gives the best result, a goodness of fit measurement inspired by Anderson (2004) is used. Other goodness of fit criteria can be found in Kristekovà

et al (2006 and 2009). Two measures are used and applied on the relative displacement, the relative speed and the relative acceleration responses. The goodness of fit measures are the cross-correlation and the ratio of peak values between the non-linear responses and the linear equivalent responses (linear oscillator of parameter f_{eq} and ξ_{eq}). We call C_{displ}, C_{speed}, C_{accel} the three cross-correlations grades and P_{displ}, P_{speed}, P_{accel} the three peak values grades:

$$C\big(a_1(t), a_2(t)\big) = \max\left(\frac{\int a_1(t)a_2(t)dt}{\sqrt{\int a_1^2 dt}\,\sqrt{\int a_2^2 dt}}\,;0\right) \tag{25}$$

$$P\big(a_1(t), a_2(t)\big) = \frac{\max\left(|a_1|\right)}{\max\left(|a_2|\right)} \tag{26}$$

The closer theses grades are to 1, the better the fit is. An example is show figure 6. The C_{accel} grades are plotted regarding the demand of ductility for thirty samples of responses in the case of wide band input motions $\gamma_i(t)$.

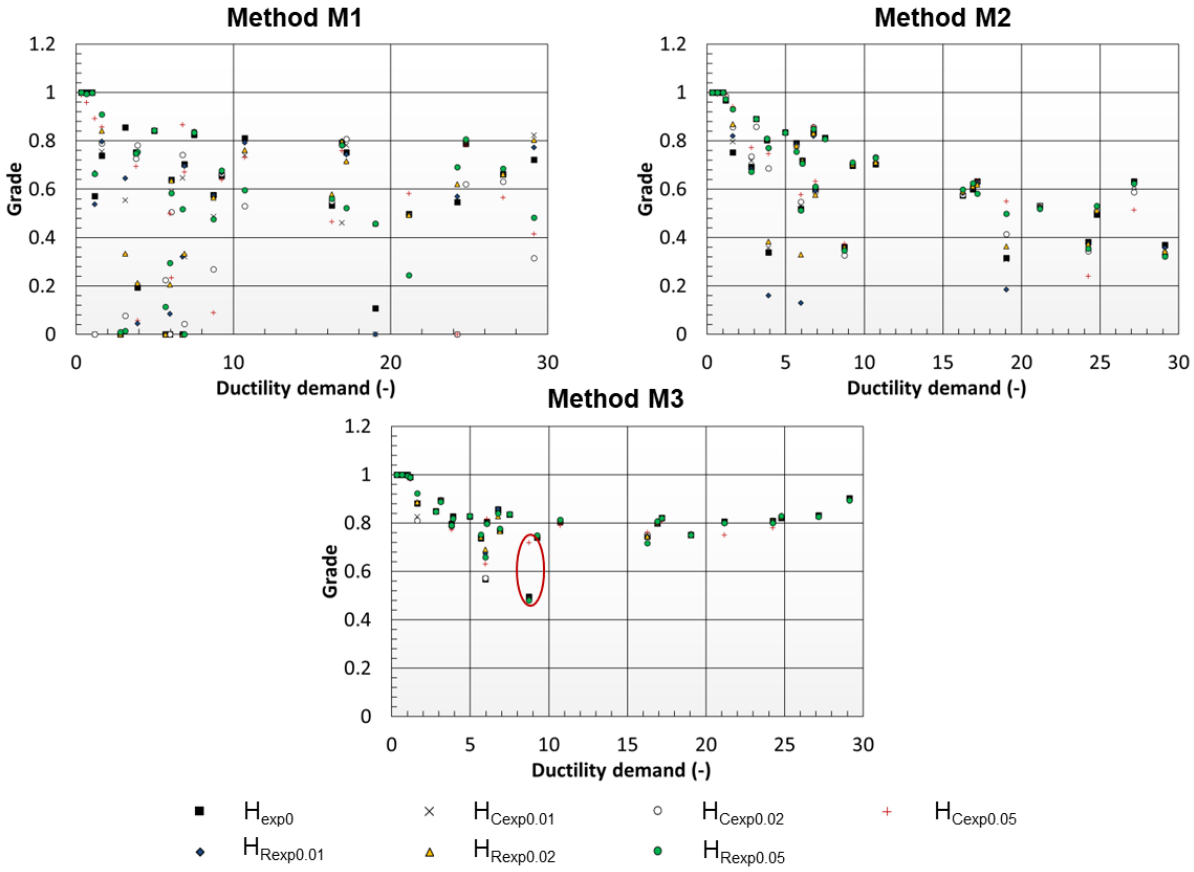

Figure 6: Relative acceleration cross-correlation grades for the M1, M2, M3 methods – Wide band input signals

From figure 6, we see that method M3 gives overall better results than the two other methods. M2 is arguably the less precise method. The red circle on the method M3 plot highlights the interest of the epsilon addition. In this case, the 5% complex epsilon gives more precise results increasing the cross-correlation grade. In consequence of these results, we study method M3 only for the rest of this study. To decide which epsilon value gives the best (f_{eq} ; ξ_{eq}) parameters set for each sample, a mean of the (26) and (27) grades is done according to this equation:

$$N = (3C_{accel} + 3C_{speed} + 0.5C_{displ} + 2P_{accel} + 2P_{speed} + 0.5P_{displ})/11 \tag{27}$$

Each epsilon value is tested, the one that has the N value the closest to 1 determines the best (f_{eq} ; ξ_{eq}) set retained. In this regard, f_{eq}/f_0 and ξ_{eq} regarding the ductility demand are plotted respectively on figures 7 and 8. The case of 1000 wide band $\gamma_i(t)$ and 1000 narrow band $\gamma_{fi}(t)$ input motions samples are explored. For each type of input motion, the case of zero-mean force and non-zero mean force equals to two-third of the yield strength are represented. For the sake of brevity, only the results for the EPP and LKH models are represented. The results are compared to the formulas proposed in Jacobsen (1930) and Liu et al.'s (2014).

Regarding the ratio f_{eq}/f_0, the results are compared to the secant stiffness formula:

$$\frac{f_{eq}}{f_0} = \sqrt{\frac{1+\alpha(d-1)}{d}} \tag{28}$$

Regarding the ξ_{eq} value, the results are compared to the Jacobsen (1930) approach developed in Liu et al.'s (2014):

$$\xi_{eq} = \xi_0 + \frac{2(1-\alpha)(d-1)}{\pi d\big(1+\alpha(d-1)\big)} \tag{29}$$

and to the Liu et al.'s (2014) formula:

$$\xi_{eq} = \xi_0 + \frac{2(1-\alpha)(d-1)}{\pi d\big(1+\alpha(d-1)\big)\big((0.7763+0.2886/f_0)+(0.5651+1.8410/f_0)/\exp(\alpha-d)\big)} \tag{30}$$

Overall, the secant stiffness formula does not predict the same equivalent frequency ratio as the RATF fit. This formula depends on the demand of ductility but does not take into account a potential non-zero mean force. As observed and as expected, the equivalent parameters curves are different in the case of non-zero mean force as, for the same dynamic level of excitations, the system has accumulated more plastic displacement than for the zero mean force case. So, for the same ductility value, the non-zero mean force case predicts a lower frequency shift ratio and a lower equivalent viscous damping ratio. Regarding the equivalent viscous damping ratio, the Jacobsen formula does not give good results. Liu et al.'s formula give better results in the case of zero mean force and wide band input signals even if it is less precise for low ductility demand and it does not predict the good asymptotic value. The predictions are less accurate for the case of narrow band signals and the formula is not adapted in the case of non-zero mean force input motions as discussed above. In the case of the LKH oscillator under non-zero mean force, we can observe a change of slope for a certain ductility demand in the evolution tendency of the equivalent parameters. This result can be explained in the sense that as discussed before, the LKH asymptotic behavior can either be elastic or plastic shakedown. But before the asymptotic state is reached, the system accumulates plastic displacement just as the EPP or the NLKH model. The first slope represents this phase whereas the second one, reached for a certain ductility demand, represents the phase when the system exhibits plastic shakedown.
Nugyen (2017) showed up the influence of the ratio f_0/f_c on the values of equivalent dynamic parameters. We can observe in figure 7 and 8 that equivalent parameters evolution tendencies are not the same when the input signal bandwidth is wide or narrow. This is another result that highlights the importance of the frequency content of the input motion on the mechanical system dynamic response. In future works, formulas for the frequency shift ratio and equivalent damping will be proposed based on the presented results.

The goodness of fit mean grades are represented in figure 9 for the EPP behavior. The blue envelope represents the perfect notation. The method gives overall good results in terms of relative speed and relative acceleration criteria. However, the displacement criteria, especially the displacement peak value, obtained poor grades. This result is not surprising, as the fit is done regarding the response RATF that does not capture the plastic drift value. Moreover, a sample of the equivalent linear oscillator relative displacement response is always zero-mean which is not the case for the non-linear oscillator. Thus, this is very unlikely to predict the peak of displacement value with the method proposed in this article. Nonetheless, the method would give good results regarding the transferred dynamic motion.

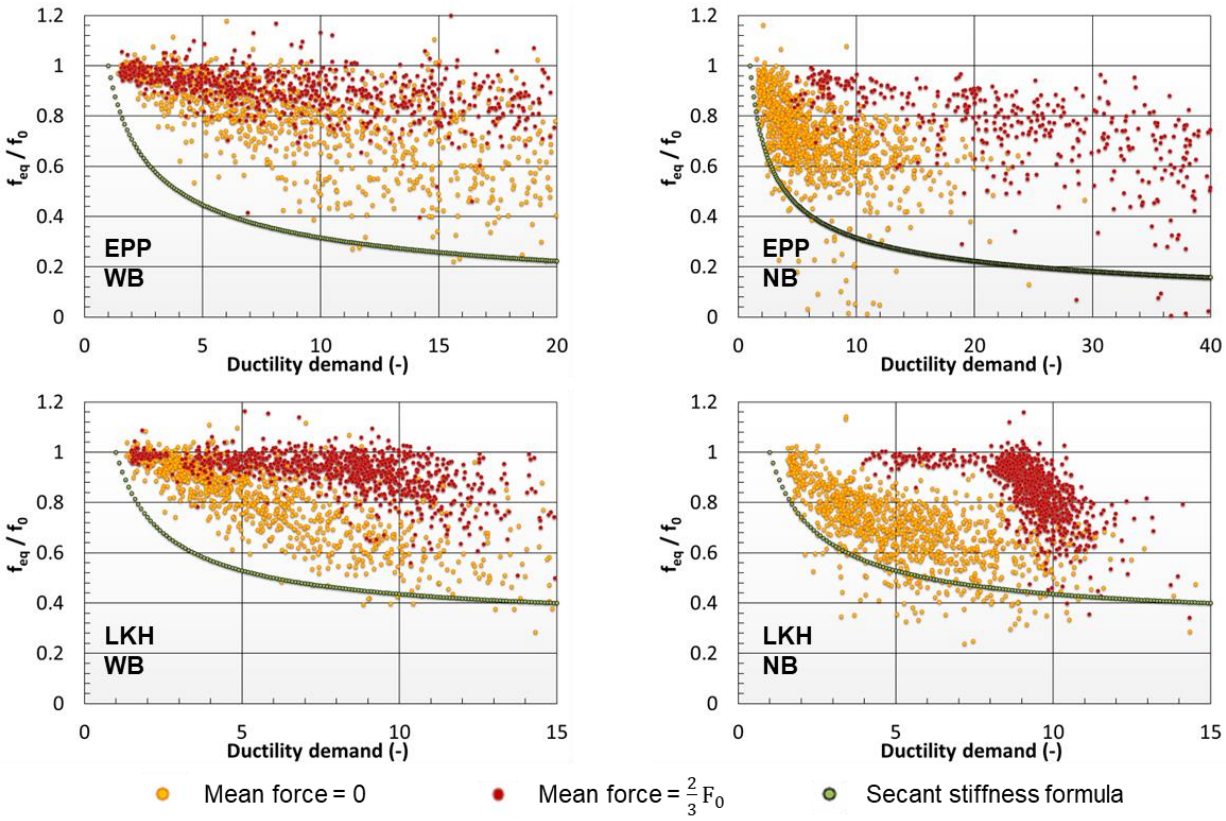

Figure 7: Equivalent frequency over natural frequency ratio regarding ductility demand for wide band (WB) and narrow band (NB) input motions

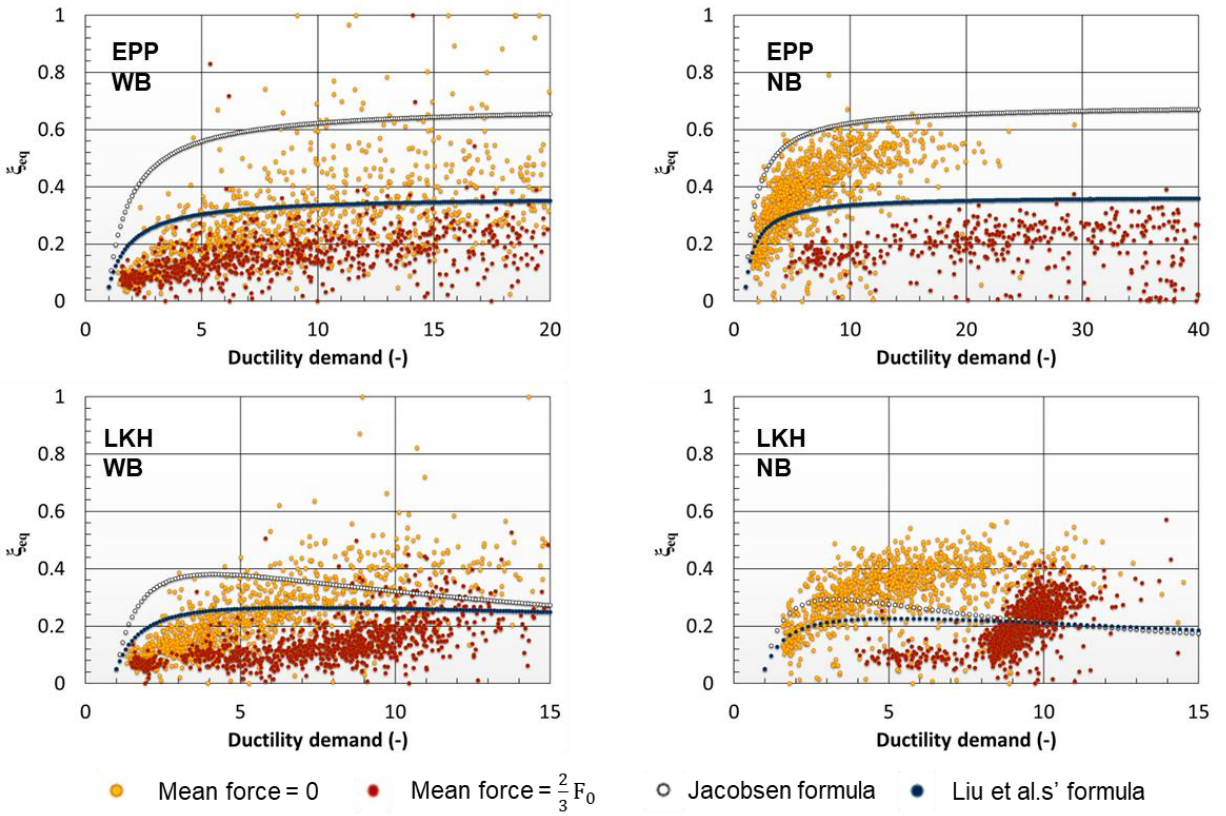

Figure 8: Equivalent viscous damping ratio regarding ductility demand for wide band (WB) ad narrow band (NB) input motions

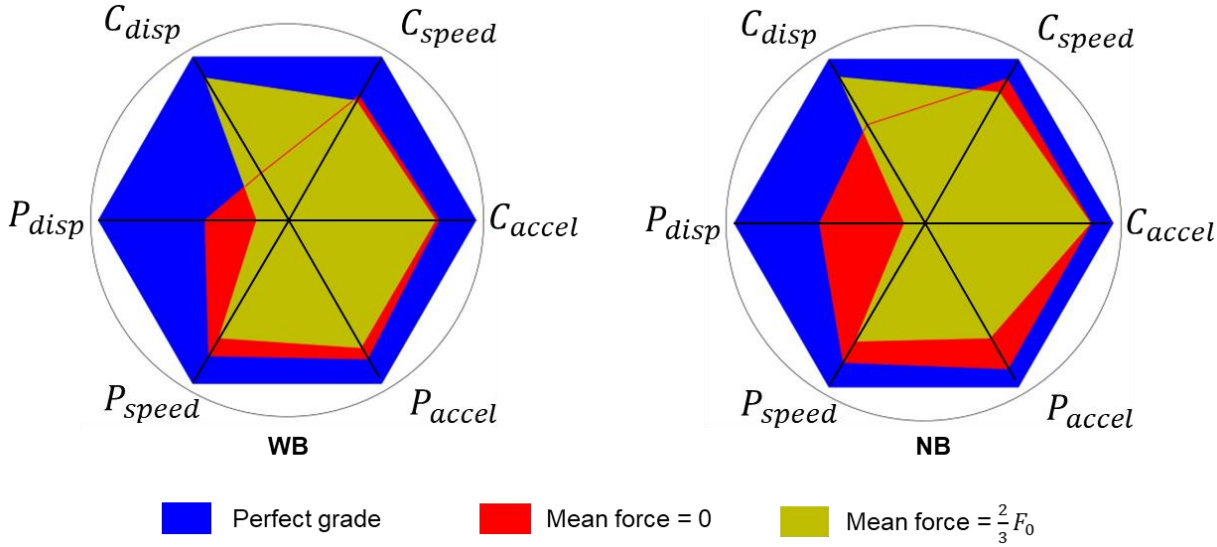

Figure 9: Mean grades in the case of the EPP oscillator for wide band (WB) and narrow band (NB) input motions

Conclusion

This paper presents an equivalent linearization method based on the fitting of the linear relative acceleration transfer function on the non-linear one to obtain the equivalent dynamic parameters f_{eq} and ξ_{eq}. This method was first introduced in Nguyen (2017). Three fitting formulas, based on the difference of the transfer function, are proposed. One is retained. An additional value has been introduced in the algorithm to improve the calculation of the non-linear numerical transfer function.

Equivalent dynamic parameters f_{eq} and ξ_{eq} versus ductility demand curves have been plotted. The influence of the input motion bandwidth has been highlighted. For the same ductility demand, the equivalent viscous damping tends to be higher for the case of narrow band signals than for the case of wide band ones. Formulas from the literature have been compared with this article fitting method. Overall, these formulas do not fit for every situation and do not take into account the frequency content of the input motions. Formulas based on the presented results will be proposed in future works.

The proposed method has been evaluated by mean of goodness of fit criteria. The relative speed and acceleration criteria showed that this article linearization method gives good results regarding these measures. However, it gives poor results regarding the prediction of the relative displacement response peak value. This assessment is tightly linked to the choice made for the fitting. Thus, the proposed linearization method should be used, for example, for the prediction of transferred input motion or for fatigue analysis.

References

1) Anderson, J.G., 2004. Quantitative Measure Of The Goodness-Of-Fit of Synthetic Seismograms, 13th World Conference on Earthquake Engineering.
2) Armstrong, P.J., Frederick, C.O., 1966. A Mathematical Representation of the Multiaxial Bauschinger Effect. CEGB, Research & Development department.
3) Blandon, C.A., Priestley, M.J.N., 2005. EQUIVALENT VISCOUS DAMPING EQUATIONS FOR DIRECT DISPLACEMENT BASED DESIGN. J. Earthq. Eng. 9, 257–278.
4) Borsoi L, Labbe P., 1989. Approche probabiliste de la ruine d'un oscillateur elasto-plastique sous séisme. 2 ème colloque national de l'AFPS. 18–20, April 1989.
5) Bouc, R., Boussaa, D., 2002. Drifting response of hysteretic oscillators to stochastic excitation. Int. J. Non-Linear Mech. 37, 1397–1406.
6) Bouc, R., Boussaa, D., 2001. Drifting response of elastic perfectly plastic oscillators under zero mean random load. Comptes Rendus Académie Sci. - Ser. IIB - Mech. 329, 323–329.

7) Bouc, R., Boussaa, D., 1998. Ratcheting response of elastic perfectly plastic oscillators under random load with non-zero mean. Comptes Rendus Académie Sci. - Ser. IIB - Mech.-Phys.-Astron. 326, 475–482.
8) Boussaa, D., Labbé, P., 1992. Seismically induced ratcheting: A probabilistic analysis of a simple case, Recent advances in earthquake engineering and structural dynamics, pp 661-678.
9) Boussaa, D., Bouc, R., 2019. Elastic perfectly plastic oscillator under random loads: Linearization and response power spectral density. J. Sound Vib. 440, 113–128.
10) Caughey, T.K., 1960. Sinusoidal Excitation of a System With Bilinear Hysteresis. J. Appl. Mech. 27, 640–643.
11) Chaboche, J.L., 1991. On some modifications of kinematic hardening to improve the description of ratchetting effects. Int. J. Plast. 7.
12) Chaboche, J.L., 1989. Constitutive equations for cyclic plasticity and cyclic viscoplasticity. Int. J. Plast. 5, 247–302.
13) Clough, R. W., and Penzien, J., 1975. Stochastic response of linear MDOF systems, Dynamics of structures, McGraw–Hill, New York.
14) Feau, C., 2008. Probabilistic response of an elastic perfectly plastic oscillator under Gaussian white noise. Probabilistic Eng. Mech. 23, 36–44.
15) Iwan, W.D., Paparizos, L.G., 1988. The stochastic response of strongly yielding systems, Probabilistic Engineering Mechanics, 1988, Vol. 3, No. 2.
16) Jacobsen, L.S., 1930. Steady Forced Vibration as Influenced by Damping: An Approximate Solution of the Steady Forced Vibration of a System of One Degree of Freedom Under the Influence of Various Types of Damping. J. Fluids Eng. 52, 169–178.
17) Jennings, P. C., Housner, G. W., and Tsai, G. W., 1968, Simulated Earthquake Motions Technical Report, Earthquake Engineering Research Laboratory, California Institute of Technology, Pasadena, California.
18) Karnopp, D., Scharton, T.D., 1966. Plastic Deformation in Random Vibration. J. Acoust. Soc. Am. 39, 1154–1161.
19) Kristeková, M., Kristek, J., Moczo, P., 2009. Time-frequency misfit and goodness-of-fit criteria for quantitative comparison of time signals. Geophys. J. Int. 178, 813–825.
20) Kristekova, M., Kristek, J., Moczo, P., Day, S.M., 2006. Misfit Criteria for Quantitative Comparison of Seismograms. Bull. Seismol. Soc. Am. 96, 1836–1850.
21) Labbé, P., June 2023, Statistical analysis of seismically induced sliding of gravity dams in European context, 91st Annual ICOLD Meeting – Gothenburg 13-14.
22) Labbé, P., 2021, Dynamique spécialisée pour les ouvrages énergétiques, Ecole des ponts ParisTech.
23) Labbé, P., 2020. On Categorization of Seismic Load As Primary or Secondary for Multi-Modal Piping Systems, in: Volume 9: Seismic Engineering. Presented at the ASME 2020 Pressure Vessels & Piping Conference, American Society of Mechanical Engineers, Virtual, Online, p. V009T09A001.
24) Labbé, P., Nguyen, T.A., 2021. Modified Response Spectrum Accounting for Seismic Load Categorization as Primary or Secondary in Multi-Modal Piping Systems, in: Volume 5: Operations, Applications, and Components; Seismic Engineering; Non-Destructive Examination. Presented at the ASME 2021 Pressure Vessels & Piping Conference, American Society of Mechanical Engineers, Virtual, Online, p. V005T08A006.
25) Labbé, P., Nguyen, T.A., 2019. FREQUENCY DEPENDENCE OF THE SEISMICALLY INDUCED DUCTILITY DEMAND IN A SDOF SYSTEM.
26) Lemaitre, J., Chaboche, J.-L., 1988. Mécanique des matériaux solides, Dunod, Second edition, BORDAS, Paris.
27) Liu, T., Zordan, T., Briseghella, B., Zhang, Q., 2014. An improved equivalent linear model of seismic isolation system with bilinear behavior. Eng. Struct. 61, 113–126.
28) Liu, T., Zordan, T., Zhang, Q., Briseghella, B., 2015. Equivalent Viscous Damping of Bilinear Hysteretic Oscillators. J. Struct. Eng. 141, 06015002.
29) Maitournam, H., 2019. Matériaux et structures anélastiques, Les éditions de l'école polytechnique, Institut Polytechnique de Paris
30) Nguyen, T.A., 2017. Analyse systématique du concept de comportement linéaire équivalent en ingénierie sismique, PhD., université Paris-Est, ESTP, Cachan.
31) Paparizos, L.G., Iwan, W.D., 1988. Some Observations on the Random Response of an Elasto-Plastic System. J. Appl. Mech. 55, 911–917.
32) Prager W., 1955. The theory of plasticity: a survey of recent achievements, Proc. Inst. Mech. Engrs. 169, 41.
33) Preumont, A., 1994. Random Vibration and Spectral Analysis, Solid Mechanics and Its Applications. Springer Netherlands, Dordrecht.
34) Reddy, C.K., Pratap, R., 2000. Equivalent Viscous Damping for a Bilinear Hysteretic Oscillator. J. Eng. Mech. 126, 1189–1196.
35) Tajimi, H. ,1960. A statistical method of determining the maximum response of a building structure during an earthquake. In Proceedings of the 2nd World Conference on Earthquake Engineering, Tokyo, Japan, pages 781–797.
36) Vanmarcke, E., 1984. Random field: Analysis and synthesis, second printing, The Massachusetts Institute of Technology.
37) Vincens, E., Labbé, P., Cambou, B., 2003. Simplified estimation of seismically induced settlements: SIMPLIFIED ESTIMATION. Int. J. Numer. Anal. Methods Geomech. 27, 669–683.
38) Yaw, P.L.L., 2017. Nonlinear Static - 1D Plasticity - Isotropic and Kinematic Hardening, Walla Walla University.